Sains Malaysiana 54(9)(2025): 2201-2210
http://doi.org/10.17576/jsm-2025-5409-08

Synthesis and Evaluation of *Para*-Substituted Bis(Arylidene)Cycloalkanones as Potential α-Amylase Inhibitor with Molecular Docking and ADMET Profiling

(Sintesis dan Penilaian *Para* Bis(arilidena)sikloalkanon Tertukar Ganti sebagai Perencat α-Amilase Berpotensi dengan Dok Molekul dan Pemprofilan ADMET)

NUR FARAH ATIQAH AZMI[1], MOHAMAD NURUL AZMI[1,*], MAHDI BABAI[1], MOHAMAD HAFIZI ABU BAKAR[2], MUNTAZ ABU BAKAR[3] & MOHAMMAD TASYRIQ CHE OMAR[4]

[1]*Natural Products and Synthesis Organic Laboratory (NPSO), School of Chemical Sciences, Universiti Sains Malaysia, 11800 Minden, Penang, Malaysia*
[2] *Bioprocess Technology Division, School of Industrial Technology, Universiti Sains Malaysia, 11800 Minden, Penang, Malaysia*
[3]*Department of Chemical Sciences, Faculty of Science and Technology, Universiti Kebangsaan Malaysia, 43600 UKM Bangi, Selangor, Malaysia*
[4] *Biological Section, School of Distance Education, Universiti Sains Malaysia, 11800 Minden, Penang, Malaysia*

Received: 15 May 2025/Accepted: 18 July 2025

ABSTRACT

Ten *para*-substituted bis(arylidene)cycloalkanone derivatives were synthesised, characterised and their inhibitory activities against human pancreatic α-amylase were evaluated. Among them, halogen-substituted derivatives **5d** (IC_{50} = 7.6 ± 1.4 μM) and **5e** (IC_{50} = 6.9 ± 1.8 μM) exhibited superior potency compared to the standard drug acarbose (IC_{50} = 23.5 ± 2.7 μM). Molecular docking studies indicated that these halogenated derivatives (i.e., compound **5d** and **5e**) showed a good interaction with human pancreatic α-amylase protein (2QV4) with binding energy of -7.4 ± 0.1 kcal/mol and -7.8 ± 0.1 kcal/mol, respectively, compared with acarbose (-3.9 ± 0.1 kcal/mol). Both of them, form crucial π–π stacking and hydrophobic interactions within the enzyme's active site residues TYR62 and LEU165. *In silico* ADMET profiling further supported the favourable drug-likeness, synthetic accessibility, and oral bioavailability of these compounds, making them promising candidates for antidiabetic drug development.

Keywords: ADMET profiling; antidiabetic agents; α-Amylase inhibitors; bis(arylidene)cycloalkanones; molecular docking

ABSTRAK

Sepuluh terbitan *para*-bis(arilidena)sikloalkanon yang tertukar ganti telah disintesis, dicirikan dan aktiviti perencatan sebatian ini terhadap enzim α-amilase pankreas manusia telah dinilai. Antaranya sebatian berhalogen, iaitu **5d** (IC_{50} = 7.6 ± 1.4 μM) dan **5e** (IC_{50} = 6.9 ± 1.8 μM), menunjukkan potensi perencatan yang lebih tinggi berbanding ubat piawai akarbosa (IC_{50} = 23.5 ± 2.7 μM). Kajian pengedokan molekul pula telah menunjukkan bahawa sebatian berhalogen (i.e., sebatian **5d** and **5e**) menunjukkan interaksi yang baik dengan protein α-amilase pancreas (2QV4) dengan tenaga pengikatan masing-masing -7.4 ± 0.1 kcal/mol dan -7.8 ± 0.1 kcal/mol, berbanding dengan acarbose (-3.9 ± 0.1 kcal/mol). Kedua-dua sebatian ini membentuk interaksi susunan π–π dan interaksi hidrofobik yang signifikan dengan asid amino TYR62 dan LEU165 di tapak aktif enzim tersebut. Analisis ADMET secara *in silico* turut menyokong ciri keberkesanan ubat yang baik, kebolehcapaian sintetik dan bioketersediaan oral bagi sebatian ini, menjadikannya calon berpotensi untuk pembangunan ubat antidiabetik.

Kata kunci: Agen antidiabetik; analisis ADMET; bis(arilidena)sikloalkanon; dok molekul; perencat α-Amilase

INTRODUCTION

Diabetes mellitus is a chronic metabolic disease characterised by persistent hyperglycaemia resulting from defects in insulin secretion, insulin action, or both (Bashary et al. 2020). Insulin, a key hormone secreted by pancreatic β-cells, is crucial in maintaining glucose homeostasis by facilitating glucose uptake from the bloodstream into peripheral tissues and regulating carbohydrate metabolism (Rahman et al. 2021). Consequently, when insulin function is impaired, glucose uptake in muscle and adipose tissues decreases while hepatic glucose production increases, leading to chronic hyperglycaemia (Fazakerley et al. 2019).

This persistent elevation in blood glucose levels disrupts metabolic homeostasis and contributes to progressive dysfunction and damage in multiple organs, including the eyes, kidneys, nerves, and cardiovascular system (Antar et al. 2023).

Among the various metabolic disturbances in diabetes, postprandial hyperglycaemia plays a critical role in early disease progression and the development of complications (Blüher, Malhotra & Bader 2023). Fluctuations in glucose levels following meals have been shown to exacerbate oxidative stress, induce inflammatory responses, and accelerate vascular damage (Caturano et al. 2025; Ma et al. 2021). A key therapeutic strategy to manage this is α-amylase inhibition, which slows carbohydrate breakdown and delays glucose absorption in the small intestine (Alp et al. 2023; Blahova et al. 2021). Enzyme inhibitors like acarbose, voglibose, and miglitol are commonly used in clinical settings to control hyperglycemia by mainly blocking glucoside; acarbose also shows some inhibitory effect against amylse (Mahdi et al. 2024a). However, gastrointestinal side effects often limit their use, including flatulence, bloating, and diarrhoea, primarily caused by the accumulation of undigested carbohydrates and subsequent bacterial fermentation in the intestine (Akmal, Patel & Wadhwa 2024).

Despite their benefits in glucose control, the adverse effects of current α-amylase inhibitors underscore the need for more effective and tolerable alternative therapeutic options. Considering this, compounds with modifiable scaffolds, such as bis(arylidene)cycloalkanones, offer a promising avenue for further exploration in antidiabetic therapy. Bis(arylidene)cycloalkanone derivatives have attracted attention in medicinal chemistry due to their diverse pharmacological properties, including anticancer, anti-inflammatory, and antimicrobial activities (Mishra et al. 2019). Structurally, these compounds consist of a cycloalkanone core with two arylidene moieties, allowing modifications that may enhance biological activity (Starostin, Freidzon & Gromov 2023). Despite their broad pharmacological potential, the inhibitory activity of bis(arylidene)cycloalkanone derivatives against α-amylase has not been systematically investigated, representing a gap in developing antidiabetic drugs.

This study investigates the potential of bis(arylidene) cycloalkanone derivatives as α-amylase inhibitors. Additionally, structure-activity relationship (SAR) analysis, molecular docking, and *in silico* ADMET profiling will be conducted to gain deeper insights into their binding interactions and pharmacokinetic properties. The findings from this study are expected to provide valuable insights into the development of novel α-amylase inhibitors with potential therapeutic value and improved safety profiles, contributing to future research on diabetes management.

MATERIALS AND METHODS

CHEMICALS AND INSTRUMENTATION

All chemical reagents and solvents used in this study were purchased from Acros Organic (USA), QRec (Asia), Sigma-Aldrich Chemical Co. (USA), and E. Merck (Germany) and were used without further purification. The chemicals utilised in the synthesis and characterisation included deuterated chloroform ($CDCl_3$), *n*-hexane, ethyl acetate, absolute ethanol (99.7%), cyclohexanone, cyclopentanone, benzaldehyde, 4-bromobenzaldehyde, 4-chlorobenzaldehyde, 4-methoxybenzaldehyde, 4-methylbenzaldehyde, and sodium hydroxide.

Synthesis progress and purity were assessed by thin-layer chromatography (TLC). It was performed on pre-coated silica gel plates (Merck 60 F_{254}) using a *n*-hexane-ethyl acetate (6:4, v/v) solvent system. The reaction progress was monitored by visualising product and reactant spots under a UV lamp (Spectroline model ENF-260C/PE, λ_{max} = 254 nm). The melting points of the synthesised compounds were determined using an open capillary tube method with a Stuart Scientific SMP10 melting point apparatus (Staffordshire, UK) within a temperature range of 25-350 °C.

All synthesised compounds were characterised using IR and NMR spectroscopy. Infrared (IR) spectra were recorded on a Perkin Elmer 2000 FTIR spectrometer (Waltham, MA, USA) in the 4000–550 cm^{-1} range. Nuclear magnetic resonance (NMR) spectroscopy was conducted using a Bruker AVN 500 MHz spectrometer (Billerica, MA, USA), where ^{1}H NMR (500 MHz) and ^{13}C NMR (125 MHz) spectra were recorded in deuterated chloroform ($CDCl_3$), with tetramethylsilane (TMS) as the internal standard. Chemical shifts are reported in ppm (δ scale), referenced to the solvent signals in $CDCl_3$ (^{1}H δ 7.26; ^{13}C δ 77.0), and coupling constants are expressed in Hz. The spectral data were processed using TopSpin 4.4.0 software (Bruker Bioscience, Billerica, MA, USA).

SYNTHESIS OF BIS(ARYLIDENE)CYCLOALKANONE DERIVATIVES

The synthesis of bis(arylidene)cycloalkanone derivatives (**4a–e** and **5a–e**) was carried out following a modified procedure based on Yusoff et al. (2022). A mixture of cyclohexanone or cyclopentanone (1.0 equiv.), 4-R-substituted benzaldehydes (2.0 equiv., where R = H, OCH_3, CH_3, Br or Cl) and a catalytic amount of NaOH (5 mol%) in ethanol (2–5 mL) were stirred at room temperature in a round-bottom flask for 1-2 h. TLC was used to monitor the reaction's progress. Upon completion, the precipitate was filtered, washed with distilled water, and recrystallised from a 2:1 (v/v) ethyl acetate/ethanol solvent system to afford the pure product. The details about the reactions and spectroscopic data are shown in supporting information.

A-AMYLASE INHIBITORY ASSAY

The α-amylase inhibitory activity was assessed by following a modified procedure (Abu Bakar et al. 2020), as previously described (Mahdi et al. 2024b; Phongphane et al. 2023; Radzuan et al. 2024). The porcine pancreas α-amylase was purchased from Sigma-Aldrich (Catalogue No. A1031). The enzyme activity was validated by the manufacturer and confirmed in-house using a control assay to ensure batch consistency before use. In brief, pancreatic α-amylase (25.0 mg) was dissolved in phosphate buffer (20 mM, pH 6.9, 50 mL). A 3,5-dinitrosalicylic acid (DNSA) colorimetric reagent was prepared by dissolving DNSA (5.0 g), sodium hydroxide (8.0 g), and sodium potassium tartrate (150.0 g) in sterilised distilled water (500 mL final volume). A 1% starch solution was prepared by dissolving 0.25 g of starch in 50 mL of sodium acetate buffer (20 mM, pH 6.9).

Stock solutions (1 mM) of the test samples (**4a–e** and **5a–e**) were prepared in chloroform (100 µL) and 1% DMSO (4.9 mL), then serially diluted (12.5-200 µM) (Mahdi et al. 2024b). The reaction mixture, consisting of the sample (100 µL), α-amylase solution (200 µL), and starch solution (100 µL), was incubated at 37 °C for 10 min. DNS reagent (300 µL) was added to terminate the reaction, followed by dilution with distilled water (300 µL). The reaction mixtures were heated at boiling temperature for 10 min, cooled, and absorbance was measured at 620 nm using a microplate reader (MPR-96, Halo, Dynamica, Australia). The IC_{50} values were calculated using non-linear regression analysis (log[inhibitor] vs. response - Variable slope model) via GraphPad Prism version 10.0 software. Acarbose and buffer served as positive and negative controls, respectively. Percentage inhibition was calculated using the equation herewith:

$$\text{Percentage inhibition (\%)} = \frac{\text{Abs. control - Abs. sample}}{\text{Abs. control}} \times 100$$

STATISTICAL ANALYSIS

Data are presented as the mean ± standard deviation (SD) of triplicate experiments. Statistical significance was evaluated using one-way analysis of variance (ANOVA) in GraphPad Prism 10.0 software, with *p*-values less than 0.05 ($*p < 0.05$) considered statistically significant. All data sets were first assessed for normality using the Shapiro-Wilk test prior to performing one-way ANOVA.

MOLECULAR DOCKING STUDIES

Molecular docking studies were conducted as described by Tan et al. (2020), with slight adjustments tailored to the current study. Initially, ligand structures were sketched using ChemDraw and subsequently geometry-optimised and energy-minimised *via* Gaussian 09 software. The crystal structure of human pancreatic α-amylase (PDB ID: 2QV4; resolution: 1.97 Å) was retrieved from the Protein Data Bank. Protein preparation involved utilising the Dock Prep tools in UCSF Chimera, which included the removal of water molecules, the addition of hydrogen atoms, and the assignment of Kollman charges to the receptor. Gasteiger charges were assigned to the ligands prior to docking.

Docking simulations were performed using AutoDock 4.2 software, employing the Lamarckian Genetic Algorithm with 100 runs per ligand. A grid box of dimensions 15.1 × 46.7 × 30.8 Å was defined around the active site, as determined using BIOVIA Discovery Studio (version 24.1.0.23298). The resulting docked conformations were ranked based on binding energy and clustered by structural similarity. All docking parameters used in this study were previously validated by Funmi et al. (2025). Ligand–protein interactions were visualised in 3D using BIOVIA Discovery Studio. Predicted inhibition constant (K_i) for each ligand was calculated from their lowest binding free energy (ΔG) values using the following equation:

$$\Delta G = RT \ln K_i$$

where R represents the gas constant (1.987 $cal \cdot mol^{-1} \cdot K^{-1}$) and T denoted temperature (298 K).

ADMET PREDICTIONS

Physicochemical and pharmacokinetic properties, including lipophilicity (Log *P*), total polar surface area (TPSA), number of rotatable bonds, bioavailability score, and drug-likeness metrics, were predicted using the SwissADME web server (Daina, Michielin & Zoete 2017), (http://www.swissadme.ch/). Additionally, toxicological endpoints (mutagenicity, tumorigenicity, reproductive toxicity, and skin irritancy) and medicinal chemistry filters (PAINS alerts, Brenk structural alerts, and synthetic accessibility scores) were assessed using DataWarrior software (version 5.0.0) (Sander et al. 2015) (https://openmolecules.org/datawarrior).

RESULTS AND DISCUSSION

SYNTHESIS OF BIS(ARYLIDENE)CYCLOALKANONE DERIVATIVES (**4a–e** AND **5a–e**)

The synthetic route for the preparation of bis(arylidene) cycloalkanone derivatives is outlined in Scheme 1. Compounds **4a–e** and **5a–e** were synthesised *via* a Claisen-Schmidt condensation, a base-catalysed aldol-type reaction between cycloalkanone and aromatic aldehydes. The structures of the synthesised bis(arylidene)cycloalkanone derivatives were confirmed by FT-IR, ^{1}H NMR, and ^{13}C NMR spectroscopies.

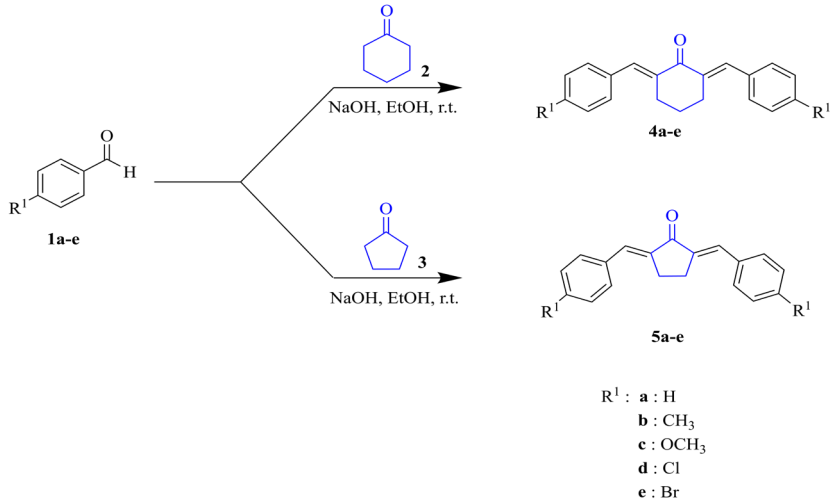

SCHEME 1. Synthesis of bis(arylidene)cycloalkanone derivatives

in-vitro α-AMYLASE INHIBITORY ACTIVITY

All synthesised and characterised bis(arylidene) cycloalkanone derivatives were evaluated for their α-amylase inhibitory activity, using acarbose as the reference standard. The IC_{50} values are summarised in Table 1 and Figure 1.

Overall, the derivatives featuring the cyclopentanone core (**5a–e**) demonstrated greater inhibitory potency than those bearing the cyclohexanone core (**4a–e**). Among them, **5d** (*para*-Cl) and **5e** (*para*-Br) exhibited the most potent inhibitory activity, with IC_{50} values of 7.6 ± 1.4 μM and 6.9 ± 1.8 μM, respectively. Both significantly outperformed the standard inhibitor acarbose (IC_{50} = 23.5 ± 2.7 μM). The remaining derivatives in this series (**5a–c**) showed moderate inhibition, with IC_{50} values comparable to or slightly better than those of acarbose.

In comparison, the cyclohexanone-based derivatives (**4a–e)** showed weaker overall inhibitory activity, although compounds **4d** (*para*-Cl) and **4e** (*para*-Br) were the most active within this series, with IC_{50} values of 19.8 ± 2.0 μM and 23.4 ± 2.5 μM, respectively. The improved activity seen with halogen substituents in both scaffolds suggests the important role of electronic effects in the *para* position. Additionally, the consistently higher potency of cyclopentanone derivatives may reflect the conformational rigidity and planarity of the five-membered ring, potentially enhancing enzyme binding (Myers et al. 2003). These results collectively highlight the importance of both the central ring scaffold and para-substituent identity in modulating α-amylase inhibition, providing a strong foundation for further structure-activity relationship (SAR) studies.

STRUCTURE-ACTIVITY RELATIONSHIP (SAR) ANALYSIS

The structure-activity relationship (SAR) analysis shows that both the core scaffold and the *para*-substituents on the arylidene moieties significantly modulate α-amylase inhibitory activity. Consistently, cyclopentanone-based derivatives (**5a–e**) exhibited greater potency than their cyclohexanone counterparts (**4a–e**), suggesting that the five-membered ring confers improved biological activity. These enhancements are likely due to the cyclopentanone system's greater planarity, which facilitates extended π-conjugation and enhances the potential for π–π stacking and hydrophobic interactions with the enzyme's active site.

Among the substituents, halogenated analogues, notably **5d** (*para*-Cl) and **5e** (*para*-Br), have the most potent inhibitory effects, with IC_{50} values of 7.62 and 6.92 μM, respectively, surpassing the standard reference acarbose (IC_{50} = 23.48 μM). Electron-withdrawing groups, such as chlorine and bromine, are known to stabilise the enone system through inductive effects without disrupting π-delocalization, thereby enhancing molecular rigidity and binding efficiency (Hage et al. 2022). Additionally, their lipophilicity facilitates interactions with the enzyme's hydrophobic regions (Verteramo et al. 2024). Interestingly, these SAR trends are corroborated by molecular docking results, which show that both **5d** and **5e** engage in favourable π-π stacking and hydrophobic interactions with key active site residues (TYR62, LEU165), located within the enzyme's hydrophobic binding pocket, as detailed in the discussion of molecular docking.

In contrast, electron-donating substituents such as methyl (**4b**, **5b**) and methoxy (**4c**, **5c**) resulted in significantly weaker inhibitory activity. These groups increase electron density over the aromatic ring system, thereby reducing the electrophilicity at the β-position of the enone system and potentially disrupting the key electronic complementarity required for optimal binding. This diminished bioactivity is consistent with weaker predicted binding interactions and lower docking scores. Overall, the SAR trends highlight the crucial role of substituent electronics, ring planarity, and hydrophobic profiles in regulating α-amylase inhibition.

These experimental observations, reinforced by docking and ADMET data, position **5d** and **5e** as promising lead scaffolds.

MOLECULAR DOCKING STUDY

To gain mechanistic insights into the observed inhibitory activity, molecular docking studies were conducted for the most active compounds, **5d** and **5e**, as well as the reference drug acarbose, against the human pancreatic α-amylase (PBD ID: 2QV4). Binding energies and inhibition constants are presented in Table 2, and key interaction profiles are summarised in Table 3.

Compounds **5d** and **5e** exhibited favourable binding energies of -7.4 ± 0.1 kcal/mol and -7.8 ± 0.1 kcal/mol, respectively, along with low predicted inhibition constants (K_i = 3.89 µM and 1.76 µM). These results indicate a strong binding affinity for the enzyme's active site. In contrast, acarbose displayed a significantly weaker binding energy (-3.9 ± 0.1 kcal/mol) and a much higher K_i (1.31 mM),

TABLE 1. IC_{50} values for α-amylase inhibitory activities

Compound	IC_{50} (µM)
4a	39.2 ± 2.1
4b	36.7 ± 2.0
4c	29.8 ± 5.6
4d	19.8 ± 2.0
4e	23.4 ± 2.5
5a	23.4 ± 2.5
5b	23.4 ± 2.5
5c	24.4 ± 2.8
5d	7.6 ± 1.4
5e	6.9 ± 1.8
Acarbose (positive control)	23.5 ± 2.7

Three independent experiments are reported with results expressed as mean ± SD (n = 3)

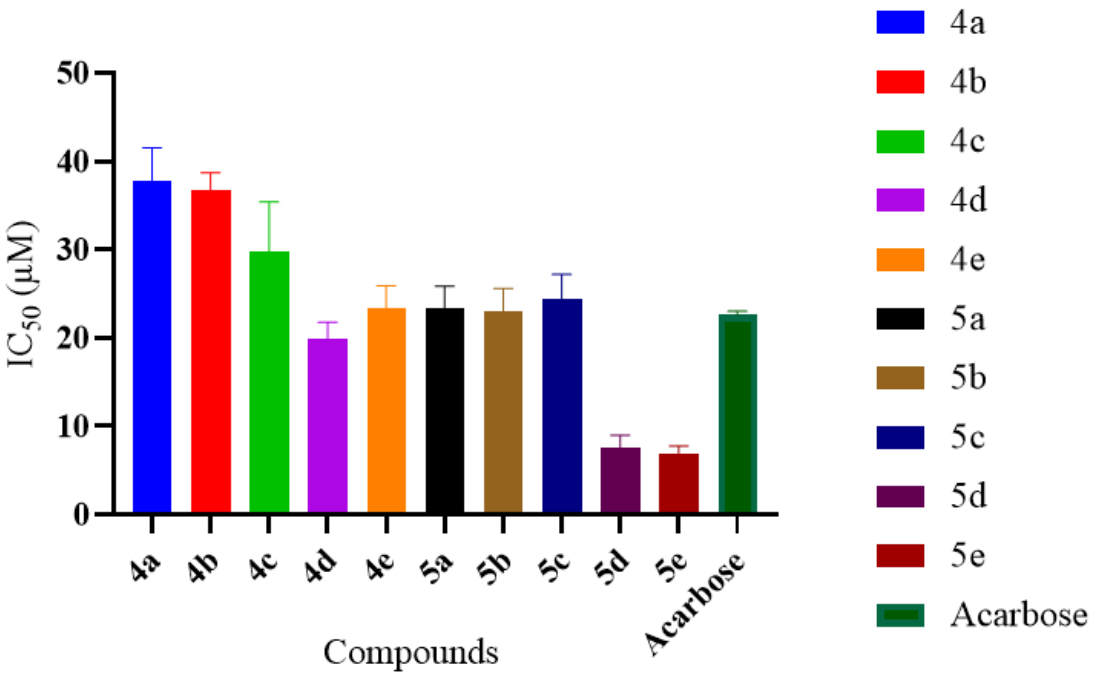

FIGURE 1. Bar graph displaying the IC_{50} values of all synthesised compounds **4** and **5** along with the reference compound acarbose

highlighting its limited interaction strength under the same docking conditions. These findings align well with the *in vitro* IC_{50} values and further validate the enhanced potency of the halogenated cyclopentanone derivatives.

Detailed interaction mapping in Table 3 shows that **5d** forms multiple non-covalent contacts, including π-π stacking and π-alkyl interactions with TYR62, an alkyl contact with LEU165, and an additional π-alkyl interaction with ALA106. Compound **5e** shares interactions with TYR62 and LEU165 but lacks contact with ALA106. Despite this, compound **5e** demonstrates stronger binding affinity, which is attributed to the high polarizability of bromine, which enables more diffuse van der Waals interactions and better shape complementarity within the hydrophobic cleft (Goel et al. 2020).

As shown in Figure 2, the 3D docking model further shows that **5e** fits compactly into the hydrophobic core of the α-amylase binding site, positioning its aromatic moieties

TABLE 2. Binding energies and inhibition constant of compounds **5d**, **5e** and acarbose with α-amylase

Compound	Binding energy (kcal mol^{-1})	Inhibition constant (μM)
5d	-7.4 ± 0.1	3.89
5e	-7.8 ± 0.1	1.76
Acarbose (control)	-3.9 ± 0.1	1.31 mM

Values are expressed as mean ± standard deviation (n = 3)

TABLE 3. Key binding interactions of compounds **5d** and **5e** and acarbose with α-amylase

Compound	Interacting unit of compound	Protein residue	Types of interaction	Distance (Å)
5d	Phenyl ring (bearing –Cl substituent)	TYR62	π–π stacked	5.34
	Phenyl ring (bearing –Cl substituent)	TYR62	π–Alkyl	4.36
	Cyclopentanone ring	LEU165	Alkyl	3.62
	Phenyl ring (bearing –Cl substituent)	ALA106	π–Alkyl	4.96
5e	Phenyl ring (bearing –Br substituent)	TYR62	π–π stacked	4.92
	Phenyl ring (bearing –Br substituent)	TYR62	π–Alkyl	4.26
	Cyclopentanone ring	LEU165	Alkyl	3.62
Acarbose	–OH group	ASP197	H-bond (Conventional)	2.33
	–OH group	ASP197	H-bond (Conventional)	1.89
	–OH group	HIS299	H-bond (Conventional)	2.13
	–OH group	ASP300	H-bond (Conventional)	1.92
	–OH group	GLN63	H-bond (Conventional)	2.31
	–OH group	THR163	H-bond (Conventional)	2.00
	C–H group	THR163	Carbon H-bond	3.36
	–OH group	ASN105	H-bond (Conventional)	2.19
	C–H group	GLU233	Carbon H-bond	2.87

near TYR62 and LEU165. This conformation promotes optimal π-π stacking and hydrophobic stabilisation, contributing to low binding energy. In contrast, **5d** adopts a slightly extended pose to accommodate the additional interaction with ALA106, near the pocket entrance (Figure 2).

Acarbose primarily binds through hydrogen bonds with the catalytic triad residues ASP197, GLU233, and ASP300 and interacts with polar residues including HIS299 (2.13 Å), GLN63 (2.31 Å), ASN105 (2.19 Å), and THR163 (2.00 Å). Additional C-H bonding is observed with THR163 (3.36 Å) and GLU233 (2.87 Å). While these interactions collectively stabilise acarbose within the enzyme's polar groove, the absence of π- or hydrophobic interactions results in a more solvent-exposed, flexible binding mode and lower overall affinity (Rahman et al. 2021).

Taken together, the docking results provide molecular-level insight into the SAR trends. They confirm that potent α-amylase inhibition arises not just from the number of interactions, but from their type, depth within the binding pocket, and overall physicochemical compatibility, all optimised in compound **5e**.

In silico ADMET AND DRUG-LIKENESS EVALUATION

In silico ADMET and drug-likeness profiling were performed to assess the pharmacokinetic potential of the lead compounds. Lipinski's rule of five (LRo5), Veber's rule, drug-likeness and bioavailability score of compounds **4a-e** and **5a-e** were assessed, Tables 4 and 5. As shown in Table 4, both **5d** and **5e** comply with Veber's rule and violate only one of Lipinski's criteria, i.e., MLogP > 4.15, which indicates good oral bioavailability. Their low total polar surface area (TPSA = 17.07 Å^2), single hydrogen bond donor (HBD = 0), and minimal rotatable bonds (n = 2) indicate favourable passive membrane permeability, supporting efficient gastrointestinal absorption (Lipinski et al. 2001; Veber et al. 2002). The drug-likeness scores of -0.17 for **5d** and -2.03 for **5e**, though slightly negative, are markedly better than acarbose (-7.40), reflecting a more favourable physicochemical profile (Walters & Murcko 2002). Furthermore, both compounds achieved a bioavailability score of 0.55, higher than acarbose's 0.17, indicating better oral administration potential (Martin 2005).

As shown in Table 5, both compounds also demonstrated low synthetic accessibility scores (2.73 for **5d** and 2.78 for **5e**), compared to acarbose (7.34), highlighting their structural simplicity and synthetic tractability. Toxicity predictions showed no alerts for mutagenicity, tumorigenicity, irritation, or reproductive toxicity. However, both **5d** and **5e** triggered a PAINS alert due to the ene-one-ene structure and a Brenk alert for the α,β-unsaturated carbonyl group (Michael acceptor). These features are commonly flagged for potential assay interference or reactivity. However, they are also essential parts of the pharmacophore responsible for α-amylase inhibition. Therefore, while these alerts suggest the need for further biological validation, they do not limit the potential for continued development.

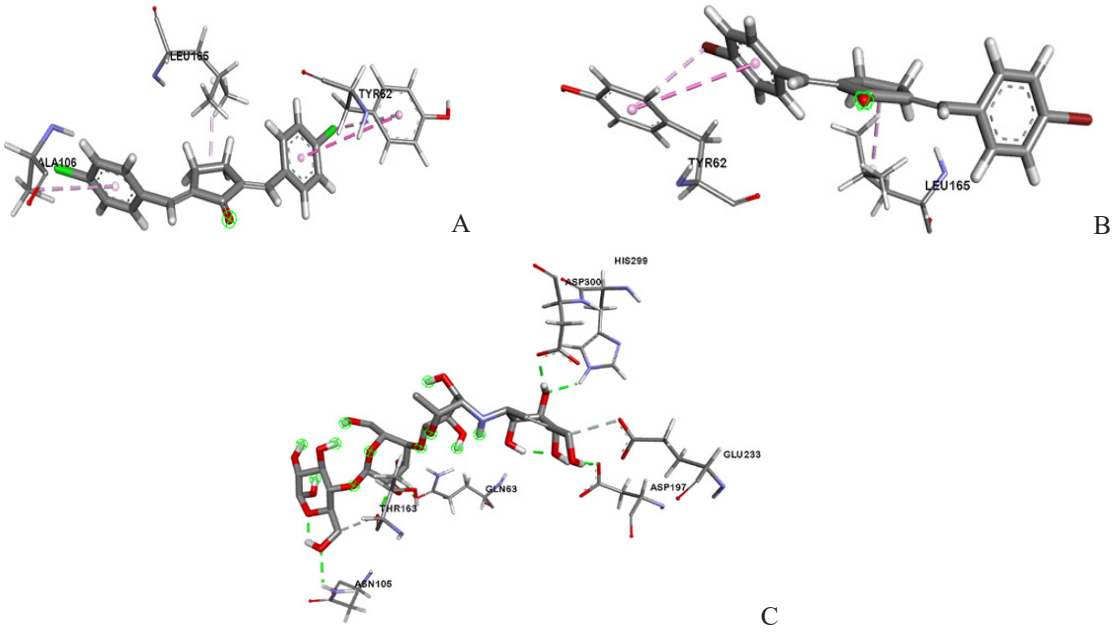

FIGURE 2. 3D binding poses of compounds **5d** (A), **5e** (B), and acarbose (C) in the α-amylase active site (PDB ID: 2QV4)

TABLE 4. Lipinski's rule of five (LRo5), Veber's rule, drug-likeness score, and bioavailability score of compounds **4**, **5** and acarbose

Compound	LRo5						Veber's rule			Drug-likeness score	Bio-availability score
	Log *P*	Mol. wt	M_NO	HBD	MLog *P*	Violation	No. rotatable bond	TPSA	Violation		
4a	3.25	274.36	1	0	4.16	1	2	17.07	0	-0.19453	0.55
4b	3.83	302.41	1	0	4.60	1	2	17.07	0	-0.21678	0.55
4c	3.86	334.41	3	0	4.71	0	4	35.53	0	-0.17345	0.55
4d	3.76	343.25	1	0	5.14	1	2	17.07	0	-0.15563	0.55
4e	4.03	432.15	1	0	5.35	1	2	17.07	0	-0.10673	0.55
5a	3.04	260.33	1	0	3.93	0	2	17.07	0	-0.14956	0.55
5b	3.56	288.38	1	0	4.92	1	2	17.07	0	-0.18456	0.55
5c	3.68	320.38	1	0	4.32	0	4	35.53	0	-0.20125	0.55
5d	3.55	329.22	1	0	4.92	1	2	17.07	0	-0.16697	0.55
5e	3.84	418.12	1	0	5.14	1	2	17.07	0	-2.034	0.55
Acarbose	1.43	645.60	19	14	-6.94	3	9	321.17	1	-7.4039	0.17

Log *P*, lipophilicity; Mol. wt., molecular weight; M_NO, number of nitrogen (N) and oxygen (O) atoms; HBD, number of hydrogen bond donor atoms; MLog *P*, predicted octanol-water partition coefficient; TPSA, total polar surface area; No. Rotatable bond, number of rotatable bonds. a) Violation of LRo5 when Log *P* > 5, molecular weight > 500, > 10 hydrogen bond acceptors, > 5 hydrogen bond donors, and MLog *P* > 4.15. b) Violation of Veber's rule when >10 rotatable bonds and > 140 Å^2 of polar surface area. Drug-likeness score: Compounds with a drug-likeness score between 2 and 7 are classified as drugs; others are considered as non-drugs (Walters & Murcko 2002)

TABLE 5. Predicted toxicity and medicinal chemistry of compounds **4**, **5**, and acarbose

Compound	Toxicity				Medicinal chemistry		
	Mutagenic	Tumorigenic	Reproductive	Irritation	PAINS	Brenk	Synthetic accessibility
4a	None	None	None	None	1 (ene-one-ene)	1 (Michael acceptor)	2.73
4b	None	None	None	None	1 (ene-one-ene)	1 (Michael acceptor)	2.97
4c	None	None	None	None	0	0	2.72
4d	None	None	None	None	1 (ene-one-ene)	1 (Michael acceptor)	2.75
4e	None	None	None	None	1 (ene-one-ene)	1 (Michael acceptor)	2.79
5a	None	None	None	None	1 (ene-one-ene)	1 (Michael acceptor)	2.73
5b	None	None	None	None	1 (ene-one-ene)	1 (Michael acceptor)	2.96
5c	None	None	None	None	0	0	2.75
5d	None	None	None	None	1 (ene-one-ene)	1 (Michael acceptor)	2.73
5e	None	None	None	None	1 (ene-one-ene)	1 (Michael acceptor)	2.78
Acarbose	None	None	None	None	0	1 (alkene)	7.34

PAINS, pan-assay interference structure; Synthetic accessibility, a score between 1 (easy to make) and 10 (very difficult to make

Overall, the ADMET and drug-likeness profiles of **5d** and **5e** support their advancement as promising, orally bioavailable α-amylase inhibitors. Their favourable absorption potential, synthetic accessibility, and safety profile, combined with their advantages over acarbose, highlight them as strong candidates for further *in vivo* studies and optimisation.

CONCLUSION

In summary, a series of *para*-substituted bis(arylidene) cycloalkanone derivatives were successfully synthesised, and evaluated as potential α-amylase inhibitors. Structure-activity relationship analysis showed that the cyclopentanone-based derivatives, particularly compounds **5d** (*para*-Cl) and **5e** (*para*-Br), exhibited

superior inhibitory activity against α-amylase compared to their cyclohexanone counterparts and the reference drug acarbose. The high potency of **5e** is attributed to its favourable electronic properties, molecular planarity, and strong π-π and hydrophobic interactions within the enzyme's active site, as confirmed by molecular docking studies. *In silico* ADMET and drug-likeness profiling further supported the pharmacokinetic suitability of both **5d** and **5e**, indicating good oral bioavailability, synthetic accessibility, and non-toxic profiles. Although structural alerts were identified due to the α,β-unsaturated carbonyl moiety, this feature is central to the compounds' inhibitory activity and warrants further evaluation. Overall, the integration of synthetic, biological, and computational data identifies **5e** as a promising lead scaffold for the development of orally active antidiabetic agents targeting α-amylase. Supplementary materials are available upon requests from the corresponding author.

ACKNOWLEDGEMENTS

The authors would like to acknowledge the financial support from the Ministry of Higher Education Malaysia (MOHE) under the Fundamental Grant Research Scheme (FRGS)-FRGS/1/2023/STG04/USM/02/3. The authors sincerely thank University Sains Malaysia (USM) and the NPSO Laboratory for the facilities used in this research work.

REFERENCES

Akmal, M., Patel, P. & Wadhwa, R. 2024. Alpha Glucosidase Inhibitors. In *StatPearls*. StatPearls Publishing.

Alp, M., Misturini, A., Sastre, G. & Gálvez-Llompart, M. 2023. Drug screening of α-amylase inhibitors as candidates for treating diabetes. *Journal of Cellular and Molecular Medicine* 27(15): 2249-2260.

Antar, S.A., Ashour, N.A., Sharaky, M., Khattab, M., Ashour, N.A., Zaid, R.T., Roh, E.J., Elkamhawy, A. & Al-Karmalawy, A.A. 2023. Diabetes mellitus: Classification, mediators, and complications; A gate to identify potential targets for the development of new effective treatments. *Biomedicine & Pharmacotherapy* 168: 115734.

Bakar, M.H.A., Lee, P.Y., Azmi, M.N., Lotfiamir, N.S., Mohamad, M.S.F., Shahril, N.S.N., Shariff, K.A., Ya'akob, H., Awang, K. & Litaudon, M. 2020. *In vitro* anti-hyperglycaemic, antioxidant activities and intestinal glucose uptake evaluation of *Endiandra kingiana* extracts. *Biocatalysis and Agricultural Biotechnology* 25: 101594.

Bashary, R., Vyas, M., Nayak, S.K., Suttee, A., Verma, S., Narang, R. & Khatik, G.L. 2020. An insight of alpha-amylase inhibitors as a valuable tool in the management of type 2 diabetes mellitus. *Current Diabetes Reviews* 16(2): 117-136.

Blahova, J., Martiniakova, M., Babikova, M., Kovacova, V., Mondockova, V. & Omelka, R. 2021. Pharmaceutical drugs and natural therapeutic products for the treatment of type 2 diabetes mellitus. *Pharmaceuticals* 14(8): 806. https://doi.org/10.3390/ph14080806

Blüher, M., Malhotra, A. & Bader, G. 2023. Beta-cell function in treatment-naïve patients with type 2 diabetes mellitus: Analyses of baseline data from 15 clinical trials. *Diabetes Obesity and Metabolism* 25(5): 1403-1407.

Caturano, A., Rocco, M., Tagliaferri, G., Piacevole, A., Nilo, D., Di Lorenzo, G., Iadicicco, I., Donnarumma, M., Galiero, R., Acierno, C., Sardu, C., Russo, V., Vetrano, E., Conte, C., Marfella, R., Rinaldi, L. & Sasso, F.C. 2025. Oxidative stress and cardiovascular complications in Type 2 diabetes: From pathophysiology to lifestyle modifications. *Antioxidants* 14(1): 72.

Daina, A., Michielin, O. & Zoete, V. 2017. SwissADME: A free web tool to evaluate pharmacokinetics, drug-likeness and medicinal chemistry friendliness of small molecules. *Scientific Reports* 7: 42717.

Fazakerley, D.J., Krycer, J.R., Kearney, A.L., Hocking, S.L. & James, D.E. 2019. Muscle and adipose tissue insulin resistance: Malady without mechanism? *Journal of Lipid Research* 60(10): 1720-1732.

Funmi, A.Z., Lim, C.Y., Ng, M.P., Toh, W.X., Tan, Y.S., Sim, K.S., Lim, S.H., Tan, C.H. & Ramle, A.Q. 2024. Investigation of cytotoxic indoleninyl-thiobarbiturate zwitterions as DNA targeting agents. *Journal of Molecular Structure* 1322: 140278.

Goel, H., Yu, W., Ustach, V.D., Aytenfisu, A.H., Sun, D. & MacKerell, A.D. 2020. Impact of electronic polarizability on protein-functional group interactions. *Physical Chemistry Chemical Physics* 22(13): 6848-6860.

Hage, K.E., Dhayalan, B., Chen, Y., Phillips, N.B., Whittaker, J., Carr, K., Whittaker, L., Phillips, M.H., Ismail-Beigi, F., Meuwly, M. & Weiss, M.A. 2025. Stabilization of a protein by a single halogen-based aromatic amplifier. *Protein Science* 34(3): e70064.

Lipinski, C.A., Lombardo, F., Dominy, B.W. & Feeney, P.J. 2001. Experimental and computational approaches to estimate solubility and permeability in drug discovery and development settings. *Advanced Drug Delivery Reviews* 46(1-3): 3-26.

Ma, C., Liu, Y., He, S., Zeng, J., Li, P., Ma, C., Ping, F., Zhang, H., Xu, L., Li, W. & Li, Y. 2021. Association between glucose fluctuation during 2-hour oral glucose tolerance test, inflammation and oxidative stress markers, and β-cell function in a Chinese population with normal glucose tolerance. *Annals of Translational Medicine* 9(4): 327.

Mahdi, B., Abu Bakar, M.H., Tasyriq, M.C.O., Zahari, A., Ibrahim, M.M., Mikhaylov, A.A. & Azmi, M.N. 2024a. Synthesis of *para*-carboxamidostilbene derivatives as antihyperglycemiaagents and their *in silico* ADMET and molecular docking studies. *ChemistrySelect* 9: e202402433.

Mahdi, B., Nurul Azmi, M., Phongphane, L., Abd Ghani, M.S., Abu Bakar, M.H., Che Omar, M.T., Mikhaylov, A.A. & Supratman, U. 2024b. Synthesis of *ortho*-carboxamidostilbene analogues and their antidiabetic activity through *in vitro* and *in silico* approaches. *Organic Communications* 17(1): 8-22.

Martin, Y.C. 2005. A bioavailability score. *Journal of Medicinal Chemistry* 48(9): 3164-3170.

Mishra, S., Das, D., Sahu, A., Patil, S., Agrawal, R.K. & Gajbhiye, A. 2019. Phosphonate derivatives of 3,5-bis(arylidene)-4-piperidone: Synthesis and biological evaluation. *Anti-Infective Agents* 18(3): 245-254.

Myers, M.C., Witschi, M.A., Larionova, N.V., Franck, J.M., Haynes, R.D., Hara, T., Grajkowski, A. & Appella, D.H. 2003. A Cyclopentane conformational restraint for a peptide nucleic acid: Design, asymmetric synthesis, and improved binding affinity to DNA and RNA. *Organic Letters* 5(15): 2695-2698.

Phongphane, L., Radzuan, S.N.M., Bakar, M.H.A., Omar, M.T.C., Supratman, U., Harneti, D., Wahab, H.A. & Azmi, M.N. 2023. Synthesis, biological evaluation, and molecular modelling of novel quinoxaline-isoxazole hybrid as anti-hyperglycemic. *Computational Biology and Chemistry* 106: 107938.

Radzuan, S.N.M., Phongphane, L., Bakar, M.H.A., Omar, M.T.C., Shahril, N.S.N., Supratman, U., Harneti, D., Wahab, H.A. & Azmi, M.N. 2024. Synthesis, biological activities, and evaluation molecular docking-dynamics studies of new phenylisoxazole quinoxalin-2-amine hybrids as potential α-amylase and α-glucosidase inhibitors. *RSC Advances* 14(11): 7684-7698.

Rahman, M.S., Hossain, K.S., Das, S., Kundu, S., Adegoke, E.O., Rahman, M.A., Hannan, M.A., Uddin, M.J. & Pang, M.G. 2021. Role of insulin in health and disease: An update. *International Journal of Molecular Sciences* 22(12): 6403.

Sander, T., Freyss, J., von Korff, M. & Rufener, C. 2015. DataWarrior: An open-source program for chemistry aware data visualization and analysis. *Journal of Chemical Information and Modeling* 55(2): 460-473.

Starostin, R.O., Freidzon, A.Y. & Gromov, S.P. 2023. Theoretical study of structure and photophysics of homologous series of bis(arylydene)cycloalkanones. *International Journal of Molecular Sciences* 24(17): 13362.

Tan, C.H., Sim, D.S.Y., Heng, M.P., Lim, S.H., Low, Y.Y., Kam, T.S. & Sim, K.S. 2020. Evaluation of DNA binding and topoisomerase I inhibitory activities of 16'-decarbomethoxydihydrovoacamine from *Tabernaemontana corymbosa*. *ChemistrySelect* 5(47): 14839-14843.

Veber, D.F., Johnson, S.R., Cheng, H.Y., Smith, B.R., Ward, K.W. & Kopple, K.D. 2002. Molecular properties that influence the oral bioavailability of drug candidates. *Journal of Medicinal Chemistry* 45(12): 2615-2623.

Verteramo, M.L., Ignjatović, M.M., Kumar, R., Wernersson, S., Ekberg, V., Wallerstein, J., Carlström, G., Chadimová, V., Leffler, H., Zetterberg, F., Logan, D.T., Ryde, U., Akke, M. & Nilsson, U.J. 2024. Interplay of halogen bonding and solvation in protein–ligand binding. *iScience* 27(4): 109636.

Walters, W.P. & Murcko, M.A. 2002. Prediction of 'drug-likeness'. *Advanced Drug Delivery Reviews* 54(3): 255-271.

Yusoff, N.M., Osman, H., Katemba, V., Ghani, M.S.A., Supratman, U., Omar, M.T.C., Murugaiyah, V., Ren, N.X., Six, Y. & Azmi, M.N. 2022. Design, synthesis, and cholinesterase inhibitory activity of new dispiro pyrrolidine derivatives. *Tetrahedron* 128: 133115.

*Corresponding author; email: mnazmi@usm.my